Graphical Abstract

To create your abstract, type over the instructions in the template box below.
Fonts or abstract dimensions should not be changed or altered.

Development of photoaffinity derivatives of the antitumor macrolide aplyronine A, a PPI-inducer between actin and tubulin

Masaki Kita,[a,b,c,*] Kota Yamagishi,[a] Kota Tsuchiya,[a] Yu Seguchi,[a] Hiroki Nakane,[a] and Hideo Kigoshi [a,*]

[a] *Graduate School of Pure and Applied Sciences, University of Tsukuba, 1-1-1 Tennodai, Tsukuba 305-8571, Japan*
[b] *Graduate School of Bioagricultural Sciences, Nagoya University, and* [c] *JST–PRESTO, Furo-cho, Chikusa, Nagoya 464-8601, Japan*

Leave this area blank for abstract info.

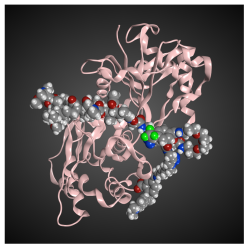

Actin–ApA probe complex

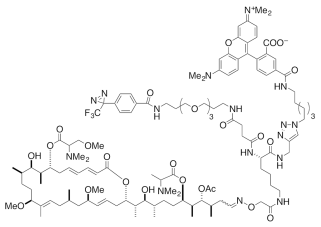

ApA–PPA–TAMRA probe

Pergamon

BIOORGANIC & MEDICINAL CHEMISTRY

Development of photoaffinity derivatives of the antitumor macrolide aplyronine A, a PPI-inducer between actin and tubulin

Masaki Kita,[a,b,c,*] Kota Yamagishi,[a] Kota Tsuchiya,[a] Yu Seguchi,[a] Hiroki Nakane,[a] and Hideo Kigoshi [a,*]

[a] *Graduate School of Pure and Applied Sciences, University of Tsukuba, 1-1-1 Tennodai, Tsukuba 305-8571, Japan*
[b] *Graduate School of Bioagricultural Sciences, Nagoya University, and* [c] *JST–PRESTO, Furo-cho, Chikusa, Nagoya 464-8601, Japan*

Received XX YY 20ZZ; revised XX YY 20ZZ; accepted XX YY 20ZZ

Abstract—The antitumor and actin-depolymerizing marine macrolide aplyronine A (ApA) synergistically binds to tubulin in association with actin, and prevents spindle formation and mitosis. While the crystal structure of the actin–ApA complex was solved in 2006, its interaction with the tubulin heterodimer has not been clarified. To investigate the binding modes of ApA as a unique protein–protein interaction (PPI)-inducer between these two cytoskeletal proteins, we prepared its photoaffinity acetylene and fluorescent derivatives with the aid of molecular modeling studies for probe design. Among these three derivatives, the ApA–PPA–TAMRA probe specifically photoreacted with both actin and tubulin *in vitro*. However, the photolabeling yield of tubulin was quite low (up to ~1%), and one of the major side-reactions was the addition of a water molecule to the carbene species generated from an aryldiazirine moiety on the hydrophilic surface of actin.

1. Introduction

The complexity and diversity of natural products lead to multiple interactions with intracellular biomolecules. Some of them have recently been shown to potently induce or inhibit protein-protein interactions (PPI). The use of PPI-stabilizing or -inhibiting scaffolds on small molecules could have important implications for simplified mimetic design, and may also provide new insight into ways to design molecules that tether proteins using different binding surfaces.[1] Therefore, the manipulation of PPI by natural products and related small bioactive molecules has become an important issue in the fields of basic research and drug discovery.[2]

Among the natural products that target cytoskeletal proteins, aplyronine A (ApA, **1**),[3–5] a 24-membered antitumor macrolide isolated from the sea hare *Aplysia kurodai*, has been shown to promote unique PPIs between actin and tubulin to interfere with microfilament dynamics (Figure 1a).[6,7] Previous studies have shown that ApA (**1**) inhibits actin polymerization by forming a 1:1 complex with the globular monomeric molecule.[8] It exhibits strong cytotoxicity against HeLa S3, a human cervical carcinoma cell line (IC_{50} 10 pM), but this concentration was much lower than that needed for disassembly of the actin cytoskeleton. To establish the modes of action and the target proteins of ApA, we have synthesized a variety of aplyronine derivatives, including biotin,[9,10] tetramethylrhodamine (TAMRA),[11] and amidopyrene [12,13] probes in combination with reactive (photoaffinity and succinyl) groups. Among these, ApA photoaffinity biotin (ApA–PB, **2**) and acetylene (ApA–PA, **4**) derivatives show potent cytotoxicity and actin-depolymerizing effects, similar to natural **1**.[14] Photolabeling experiments with probe **2** in tumor cells and subsequent affinity purification and immunoblotting analysis resulted in the identification of tubulin as the secondary target of ApA.[15] While actin and ApA alone each had little effect on tubulin polymerization *in vitro*, their 1:1 complex delayed the nucleation and growth phases, and reduced the final polymer mass of tubulin. The PPI-inducing effect of ApA (**1**) between actin and tubulin has also been supported through the use of gel-permeation HPLC [15] and surface plasmon resonance analyses.[10] Tubulin is a polymerizing cytoskeletal protein that forms microtubules, which regulate important cellular processes such as cell motility, neuronal pathfinding, cell division, and cortical flow.[16] Tubulin-targeting agents have been widely used in cancer chemotherapy,[17,18] but there are no previous descriptions of microtubule inhibitors that synergistically bind to tubulin in association with actin and affect microtubule assembly. To better understand the binding modes and antitumor mechanism of **1**, we designed and prepared ApA photoaffinity derivatives with the aid of molecular modeling studies, and performed photolabeling experiments with actin and tubulin.

Keywords: photoaffinity probe; protein–protein interaction; antitumor natural products; actin; tubulin.

* Corresponding authors. e-mail: mkita@agr.nagoya-u.ac.jp (M.K.), kigoshi@chem.tsukuba.ac.jp (H.K.)

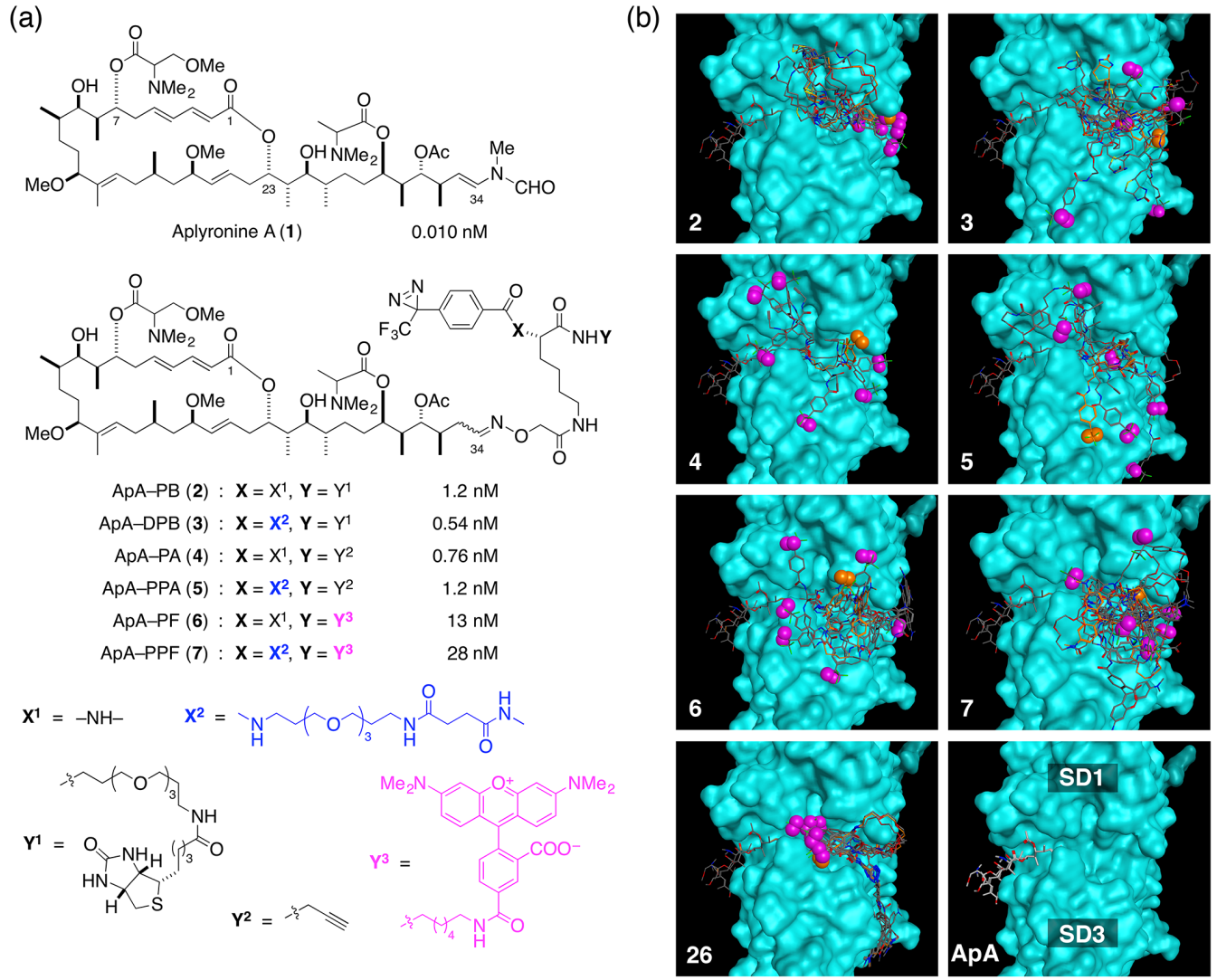

Figure 1. Structures of aplyronine A photoaffinity probes and their complexes with actin obtained by molecular modeling. (a) Structures of aplyronine A and its photoaffinity derivatives. IC_{50} values for cytotoxicity against HeLa S3 cells are shown below each compound (to the right). PEG linker (**X**^{2}) and TAMRA (**Y**^{3}) groups are highlighted in blue and pink, respectively. (b) Molecular modeling of the complexes of actin–ApA photoaffinity probes. The initial structures of the actin–probe complexes were constructed by replacing the C34 *N*-methylenamide moiety in **1** in the X-ray structure of the actin–ApA complex (PDB code: 1WUA, right bottom). Conformational searches were performed using the Amber12-EHT force-field, in which both actin and the ApA moiety (C1–C32) in probes were fixed. In each model, seven representative conformers of ApA probes within 10 kcal/mol are superimposed, which cover the distribution of diazirine moiety as much as possible on the surface between SD1 and SD3 of actin. The orange and magenta spheres represent the diazirine *N* atoms of the most stable conformer and the other six conformers, respectively.

2. Results and Discussion

2.1. Design of aplyronine A photoaffinity fluorescent devivatives

The aryltrifluoromethyldiazirine [19,20] (photoreacting) group in ApA–PB (**2**) is close to the side-chain (C23–C34) of ApA, which interacts with the hydrophobic cleft of actin. Thus, to enhance the flexibility of the photoreacting group, ApA double- polyethylene glycol (PEG)-linked photoaffinity biotin probe (ApA–DPB, **3**) was prepared.[15] Treatment with **3** increased the amounts of both photolabeled tubulin and actin *in vitro*, compared to treatment with **2**. However, due to the low detectable sensitivity and difficulty in the purification of photolabeled probes, the binding positions with these probes on tubulin were not determined. Meanwhile, photolabeling of actin with ApA–PA (**4**) proceeded highly efficiently, and the actin–probe **4** conjugate was successfully labeled with TAMRA-linked azide via Cu(I)-catalyzed 1,3-dipolar cyclization (Huisgen reaction).[21] Therefore, to determine the binding sites on tubulin, we designed an ApA PEG-linked photoaffinity acetylene derivative, ApA–PPA (**5**), which has an extended and flexible PEG linker to enable the photoreacting group to reach tubulin, as with **3**. To improve the yield and specificity of the fluorescence

labeling of tubulin with ApA probes, we considered two approaches; 1) photolabeling of tubulin with acetylene probes and subsequent *in situ* 1,3-dipolar cyclization with TAMRA azide; and 2) conjugation of the TAMRA group prior to the photoreaction with proteins. To conduct the latter experiments, we planned to synthesize an ApA photoaffinity fluorescent probe, ApA–PF (**6**), and its PEG-linked derivative, ApA–PPF (**7**).

Figure 1b summarizes the results of molecular modeling studies of the actin–ApA photoaffinity probe complexes. ApA bears a C24–C34 side chain moiety that includes a terminal *N*-methyl enamide group and two amino acid esters (*N*,*N*,*O*-trimethylserine and *N*,*N*-dimethylalanine). X-ray analysis of the actin–ApA complex revealed that **1** intercalates into the hydrophobic cleft between subdomains (SD) 1 and 3 of actin by using the side-chain moiety of **1**.[22] Thus, conformational analyses of ApA probes on actin were performed by fixing both actin and the ApA moiety (C1–C32) in each probe. Previous structure-activity relationship studies revealed that aplyronine C, a natural congener of **1** that lacks the C7 ester moiety, binds to actin but not to tubulin, and its cytotoxicity is ~2,000 times weaker than that of **1**.[3] Thus, it has been assumed that the positively-charged C7 trimethylserine ester group that protrudes from the actin–ApA complex might generate a unique tubulin-binding site on the actin–ApA complex, driving the interaction with tubulin α/β-heterodimer.[15] Comparison of the optimized structures for an actin–photoaffinity probe complex revealed that a much greater area of the actin surface was covered by the diazirine group of ApA–DPB (**3**) than that of ApA–PB (**2**), and the diazirine group in **3** was expected to more efficiently bind to tubulin. In the cases of acetylene derivatives, the diazirine groups of ApA–PA (**4**) and ApA–PPA (**5**) similarly covered a wide surface area of actin, as in probe **3**. This might be due to the small size and non-polar nature of the acetylene group, which interacts very little with the surface functional groups on actin. As for photoaffinity fluorescent derivatives, the diazirine moieties in probe **6** had a distribution similar to that as **3**, while those in probe **7** were rather restricted. This might be due to the steric repulsion between TAMRA and the PEG chain moieties on the actin surface.

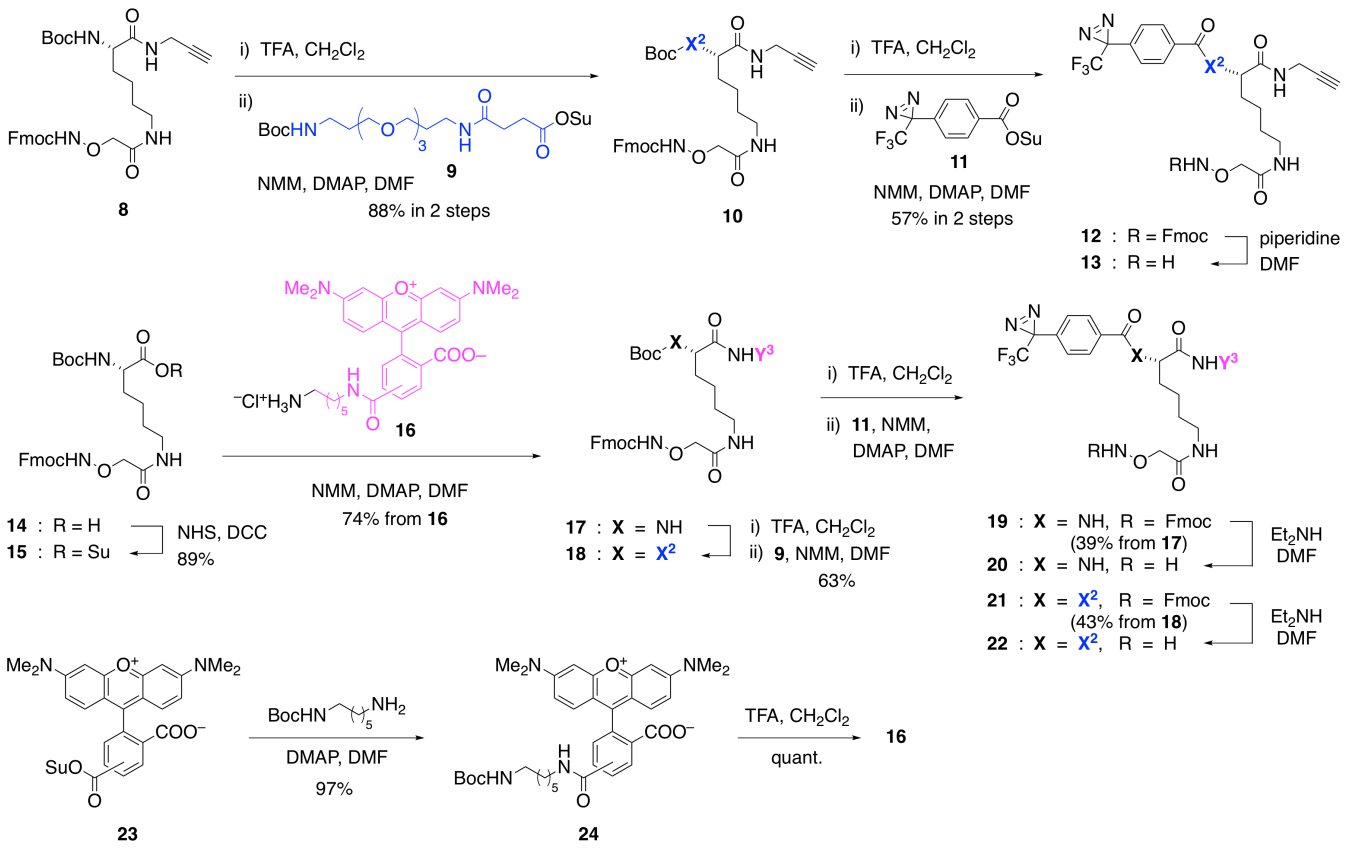

Scheme 1. Preparation of diazirine-containing alkoxyamine linkers and ApA photoaffinity derivatives. (a) Preparation of acetylene derivative **13**. (b) Preparation of TAMRA derivatives **20** and **22**. (c) Preparation of TAMRA amine **16**.

2.2. Synthesis and biological activity of aplyronine A photoaffinity fluorescent derivatives

Scheme 1 summarizes the synthesis of three diazirine-containing alkoxyamines **13**, **20**, and **22**. Acidic cleavage of the Boc group in **8** [14] derived from L-Lys with trifluoroacetic acid (TFA) followed by the coupling with PEG-linked succinyl ester **9** [15] in the presence of *N*-methylmorpholine (NMM) and 4-dimethylaminopyridine (DMAP) yielded PEG-linked amide **10** (88%). The second removal of the Boc group and condensation with succinyl ester **11** in the presence of NMM and DMAP gave aryldiazirine amide **12** (57%). Removal of the fluorenylmethyloxycarbonyl (Fmoc) group in **12** with piperidine in *N*,*N*-dimethylformamide (DMF) afforded alkoxyamine **13** in quantitative yield. On the other hand, succinyl ester **15** was prepared from L-Lys-derived carboxylic acid **14** [14] in 89% yield by conjugation with *N*-hydroxysuccinimide (NHS) and *N*,*N*′-dicyclohexylcarbodiimide (DCC).

TAMRA-conjugated amine hydrochloride **16** was prepared by the elongation of amine linker in commercially available succinyl ester **23** and removal of the Boc group in amide **24**. Coupling of **15** with TAMRA-conjugated amine hydrochloride **16** using NMM and DMAP afforded amide **17** (74%). As in the preparation of **10**, removal of the Boc group in **17** and coupling with **9** yielded PEG-linked amide **18** (63%). Both TAMRA-conjugated amides **17** and **18** were converted to aryldiazirine amides **19** (39%) and **21** (43%), respectively, the Fmoc groups of which were removed with diethylamine in DMF to provide alkoxyamines **20** and **22** quantitatively, respectively. Since all three neutral alkoxyamines **13**, **14**, and **19** were unstable, they were immediately used in the next coupling reactions with aldehydes.

With diazirine linkers in hand, we synthesized acetylene or fluorescent group-conjugated photoaffinity derivatives of ApA (**1**) (Scheme 2). Based on the finding that the C34 enamide moiety of **1** can be replaced with hydrogen bond acceptors (i.e., imines and hydrazones) without a significant loss of activity,[11] acidic hydrolysis of the *N*-methyl enamide moiety of natural **1** afforded the C34 aldehyde **25**,[9] which was condensed with alkoxyamine **13** in EtOH with the addition of acetate buffer (pH 4.0) to give ApA–PPA (**5**) (24%). Similarly, condensation of aldehyde **25** with alkoxyamines **20** and **22** afforded ApA–PF (**6**) (41%) and ApA–PPF (**7**) (61%), respectively. ApA–PPA (**5**) potently inhibited the growth of HeLa S3 cells (IC_{50} 1.2 nM), and its effects were comparable to those of previously synthesized photoaffinity derivatives **2**–**4** (IC_{50} 0.54~1.2 nM) (Figures 1a and S4). Also, ApA–PPA (**5**) strongly inhibited F-actin sedimentation, as with natural **1**, which was confirmed by ultracentrifugation (Figure S1).[11] While the TAMRA-conjugated analogs ApA–PF (**6**) and ApA–PPF (**7**) were ca. 10 and 23 times less cytotoxic than **5**, all three photoaffinity derivatives were expected to have similar affinities for actin to form a 1:1 complex, and to induce the PPI between actin and tubulin.

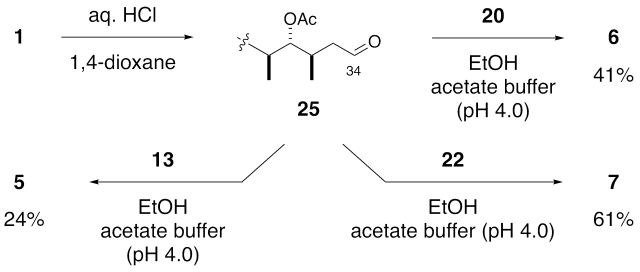

Scheme 2. Synthesis of ApA photoaffinity derivatives.

2.3. Photolabeling experiments with ApA–PPA (5)

Next, photolabeling experiments of actin and tubulin were conducted using ApA–PPA (**5**). After covalent bond formation by irradiation with UV (365 nm) at 0 °C for 30 min in a monomeric actin-stabilizing buffer, called G-buffer [2 mM Tris·HCl (pH 8.0), 0.2 mM $CaCl_2$, 0.2 mM ATP, 0.5 mM 2-mercaptoethanol], the protein–probe conjugates were further reacted with TAMRA–azide by the Huisgen reaction. In the case of actin alone, highly fluorescent protein bands were observed when the 1,3-dipolar reactions were performed for 30 min at room temperature, as with the use of ApA–PA (**4**) (Figure 2a, *lane 1* and Figure S2a).[14] On the other hand, neither the TAMRA conjugates of tubulin alone nor those of the 1:1 mixture of actin/tubulin were detected by sequential photolabeling with probe **5** / *in situ* fluorescent dye conjugation (*lanes 2 and 3*). As mentioned above, probe **5** shows potent cytotoxicity in tumor cells comparable to those of other PPI-inducing ApA derivatives, such as ApA–DPB (**3**), which highly efficiently forms a covalent bond with both actin and tubulin. Since actin-labeling by probe **5** was not observed in the presence of tubulin, the salts contained in protein tubulin might inhibit the Cu(I)-promoted Huisgen reaction.

To improve the labeling efficiency of tubulin, TAMRA dye was then conjugated to ApA–PPA (**5**) prior to the photoreaction. The Huisgen reaction between the alkyne in **5** and TAMRA–azide using sodium ascorbate, copper(II) sulfate, and tris[(1-benzyl-*1H*-1,2,3-triazol-4-yl)methyl] amine (TBTA) [23] in CH_2Cl_2–H_2O (1:1) gave ApA–PPA–TAMRA (**26**) in 19% yield (Figure 2c). Upon treatment with **26** in G-buffer, a very strong fluorescent band of actin (~43 kDa) and a weak fluorescent band of tubulin (~50 kDa) were detected (Figure 2b, *lane 1*). While the former band almost disappeared in the presence of excess **1**, the latter did not (*lane 2*). Since tubulin was expected to be too unstable to interact with actin–ApA complex in G-buffer, photolabeling might occur non-specifically on the surface of denatured proteins. Meanwhile, in a tubulin-stabilizing buffer, called BRB buffer [80 mM PIPES·Na (pH 6.9), 2 mM $MgCl_2$, 0.5 mM EGTA, 10 μM DAPI], photolabeled actin and tubulin bands were detected to the same extent, and the labeling of both proteins was significantly inhibited by excess **1** (*lanes 3 and 4*, and Figure S3). This highly specific photolabeling of actin and tubulin in the same BRB

buffer was also observed with the use of aplyronine A photoaffinity biotin probes **2** and **3**.[15] Based on the fluorescence intensity of the gel images, the photolabeling yield of tubulin with probe **26** was estimated to be ~1%.

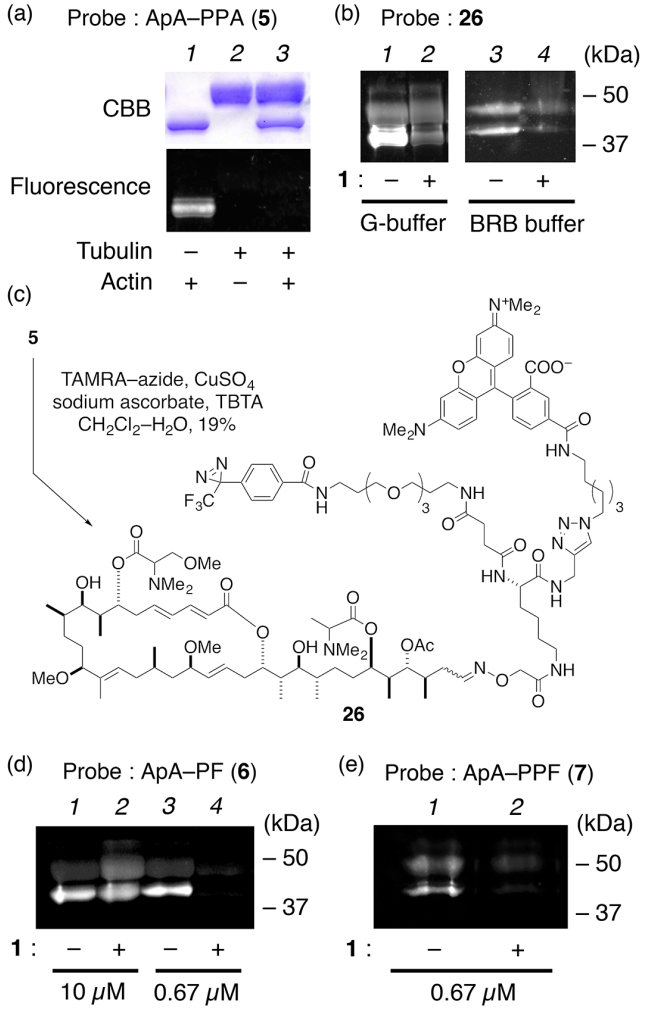

Figure 2. Photolabeling experiments for actin and tubulin with ApA probes. (a) After actin (10 μM) and/or α/β-tubulin (10 μM as a heterodimer) was incubated with ApA–PPA (**5**) (20 μM) in G-buffer, samples were irradiated with UV_{365} at 0 °C for 30 min. Photolabeled proteins were then reacted with TAMRA–azide, sodium ascorbate, $CuSO_4$, and TBTA at room temperature for 30 min. Labeled actin was detected by TAMRA fluorescence and Coomassie brilliant blue (CBB) stain. (b) Photolabeling of actin and tubulin with probe **26** in the absence or presence of excess **1**. The buffers used are shown below. (c) Preparation of triazole **26** by the Huisgen reaction. (d, e) Photolabeling of actin and tubulin with ApA–PF (**6**) or ApA–PPF (**7**) in BRB buffer in the absence or presence of excess **1**. Protein concentrations are shown below.

Molecular modeling of the actin–probe **26** complex suggested that **26** shows almost a single conformer on the surface of actin (Figure 1b). Diazirine groups of both probes **26** and ApA–PB (**2**) were highly localized between SD1 and SD3 of actin, but their positions were quite different from each other. The PEG linker parts of almost all conformers in **26** specifically interacted with the ε-amino group on Lys^{113} on actin, which might limit the positions of diazirine, triazole, and TAMRA groups. Among the most stable conformations of ApA probes, the distance between the diazirine carbon and the ApA C34 oxime carbon in **26** was shorter (7.6 Å) than those in the others (11.9~17.2 Å), which might contribute to the relatively high photolabeling efficiency for tubulin.

2.4. Photolabeling experiments with ApA–PF (6) and ApA–PPF (7)

For comparison, photolabeling experiments with actin and tubulin were performed with two photoaffinity fluorescent probes, ApA–PF (**6**) and ApA–PPF (**7**). Both probes highly effectively and specifically photolabeled actin alone in G-buffer (Figure S2b). In the case of actin–probe **6**–tubulin ternary complex in BRB buffer, actin was predominantly photolabeled with **6**, but the labeling efficiency of tubulin was fairly low (Figure 2d, *lane 1*), as with the shorter linker probes ApA–PB (**2**) and ApA–PA (**4**). Moreover, as opposed to the results with the use of **26**, competitive inhibition by ApA (**1**) was unsuccessful at protein concentrations of 10 μM (*lane 2*). After several attempts, a 15-fold dilution of probe **6** and proteins resulted in the specific photolabeling of actin and tubulin (*lanes 3 and 4*). ApA–PPF (**7**) also specifically photoreacted with both actin and tubulin at the same diluted concentration, but its photolabeling efficiency for tubulin was not any better than those of **26**.

To consider the reason for the low photolabeling yields of ApA fluorescent probes, photoreacted actin with ApA–PF (**6**) was ultrafiltered, the proteins in retentate fractions were digested with trypsin, and the tryptic peptides were analyzed by fluorescent LC-MS (Figure 3a). The dominant fluorescent product was not the photoreacted tryptic peptide–probe **6** conjugates, but rather the water adduct to the carbene moiety generated by photolysis of the trifluoromethylaryldiazirine moiety in **6** (Figure 3d).[24] This water adduct completely disappeared when photoreacted actin was denatured with 2 M guanidine (Figure 3b) or treated with an excess amount of ApA (**1**) (Figure 3c) before ultrafiltration. Apart from the hydrophobic binding of the side-chain moiety (C24–C33), the C34 terminal *N*-methyl enamide in **1** is located in a hydrophilic environment and interacts with the water molecules inside of the actin–ApA complex.[22] Thus, probe **6** might easily photoreact with a water molecule on the surface of actin, and the water adduct might still tightly bind to actin. During the fluorescent LC-MS analysis of the photolabeled products of tryptic actin peptide–probe **6** conjugates, several minor fluorescent peaks were detected in addition to the water adduct, but no specific mass peaks of photolabeled peptides were detected due to the low photolabeling efficiency. Among tested, BRB buffer gave the best result for the photolabeling experiments of tubulin, and the low photolabeling efficiency of ApA derivatives might be due to the position of photoreacting groups on the ApA probes as well as the hydrophilic properties of the ApA-binding sites on the target proteins.

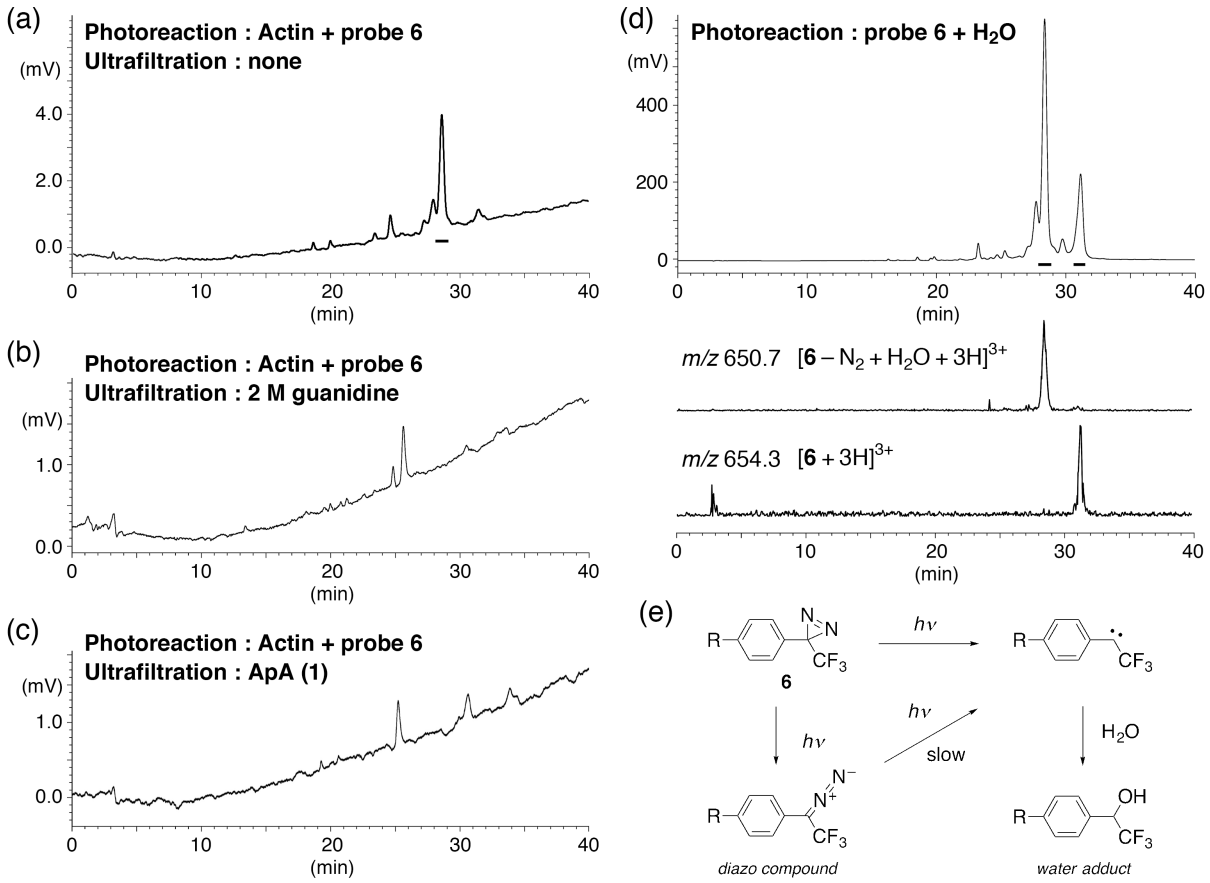

Figure 3. Fluorescence LC-MS analysis of digested actin photoreacted with ApA–PF (**6**). HPLC conditions: Column, Develosil RP-AQUEOUS AR-5 (1.5 mm I.D. × 150 mm); Eluate, 10–70% MeCN / 0.05% TFA aq. (linear gradient for 40 min); Flow rate, 0.1 mL/min; Temp. 25 °C, Detection, fluorescence λ_{ex} 565 nm, λ_{em} 580 nm. (a–c) After the photolabeling experiments, samples were ultrafiltered (14,000 × *g*, 4 °C, 15 min, MWCO 10 kDa, three times). The proteins in retentate fractions were carbamidomethylated and digested with trypsin, and the tryptic peptides were analyzed. In (b), photoreacted actin was denatured with 2 M guanidine before ultrafiltration. In (c), photoreacted actin was treated with excess **1** before ultrafiltration to competitively remove the probe derivatives that did not react with actin. (d) LC-MS analysis of probe **6** that photoreacted with water. The two mass chromatograms on the bottom correspond to the water adduct (t_R 28.4 min) and unreacted **6** (or a diazo compound, t_R 31.0 min), respectively. The water adduct was also observed in (a) as a major peak. (e) Photolysis scheme for the trifluoromethylaryldiazirine moiety in **6**.

3. Conclusion

In summary, we have developed photoaffinity derivatives of the antitumor macrolide aplyronine A, a unique PPI inducer between actin and tubulin. To investigate the binding modes of ApA to these two cytoskeletal proteins, we prepared its photoaffinity acetylene and fluorescent derivatives **5**–**7** with the aid of molecular modeling studies for probe design. The most successful tubulin photolabeling *in vitro* was achieved with the use of an ApA–PPA–TAMRA probe **26**; However, the photolabeling yield of tubulin was quite low (up to ~1%), and we could not identify its binding site on tubulin. Further investigations on the protein conjugation reaction for minute and labile targets, including a binding-position analysis by MS, and the mechanisms of action of aplyronines and related PPI-inducing marine macrolides are currently underway.

4. Experimental

4.1. Cell culture and cytotoxicity assay

HeLa S3 cells (suspension culture-adapted human cervical carcinoma cell line, ATCC CCL-2.2) were cultured in Eagle's minimal essential medium (E-MEM) supplemented with fetal bovine serum (FBS, 10%) in a humidified atmosphere containing CO_2 (5%). ApA (**1**) was isolated from the sea hare *Aplysia kurodai*, according to published methods.[3,5] For bioassays, ApA and its photoaffinity derivatives were stored in DMSO at 1 mM, unless otherwise noted. The cytotoxicity of ApA and its derivatives were measured by the 3-(4,5-dimethylthiazol-2-yl)-2,5-diphenyl tetrazolium bromide (MTT) method. In brief, HeLa S3 cells were seeded at 2×10^3 cells per well in 96-well plates. After incubation overnight at 37 °C, aplyronines (1 pM – 1 μM) were added, and the cells were incubated for 96 h at 37 °C.

4.2. *In vitro* F-actin sedimentation assay

To a solution of rabbit skeletal muscle actin (3 μM, Cytoskeleton) in G-buffer [2 mM Tris·HCl (pH 8.0), 0.2 mM $CaCl_2$, 0.2 mM ATP, 0.5 mM 2-mercaptoethanol] (500 μL) was added a 0.15 M solution of $MgCl_2$ (3.3 μL), and the mixture was stirred at 25 °C for 1 h.[11] To the solutions of F-actin were added samples (3 μM), and the resulting mixtures were stirred at 25 °C for 1 h and then ultracentrifuged (150,000 × *g*, 22 °C, 1 h). The supernatants (lyophilized) and the precipitates were dissolved in 1 × SDS buffer (100 μL, Sigma) and boiled at 95 °C for 5 min. SDS-PAGE was performed by using a precast 10% polyacrylamide gel (ATTO), and the gels were stained with a Quick-CBB kit (Wako).

4.3. Photolabeling and fluorescent labeling experiments with photoaffinity acetylene probes

To protect aryl diazirine derivatives from light, all experiments were conducted with light-shaded glass or plastic equipment, or under a yellow-filtered light hood. For actin labeling experiments with photoaffinity acetylene derivatives (Fig. S2a), actin (0.24 nmol, from rabbit skeletal muscle, Sigma Co.) was incubated with ApA–PPA (**5**) or ApA–PA (**4**) (0.48 nmol each) in a 1:11 mixture of DMSO / G-buffer (24 μL) in 0.6 mL Eppendorf tubes at 0 °C for 30 min, as mentioned previously.[14] For actin and tubulin labeling experiments with ApA–PPA (**5**) (Fig. 2a), actin from rabbit skeletal muscle (0.48 nmol) and/or tubulin (0.48 nmol as a heterodimer) prepared from porcine brain using high-molarity buffer [25] were incubated with **5** (0.96 nmol) in a 1:22 mixture of DMSO / G-buffer (46 μL, containing ~10 times diluted tubulin buffer salts) in 0.6 mL Eppendorf tubes at 0 °C for 30 min. UV irradiation was carried out at 0 °C for 15 min by using a handy UV lamp (365 nm, 0.8 mW/cm^2), and solutions of TAMRA–azide (1 mM, 1 μL, 1 nmol) and TBTA (10 mM, 1 μL) in DMSO and aqueous solutions of sodium ascorbate (14 mM, 1 μL) and copper(II) sulfate (10 mM, 1 μL) were then added. The reaction mixture was incubated at room temperature for 30 min, quenched with an equal volume of 2 x SDS-buffer and boiled at 95 °C for 5 min. SDS-PAGE was performed by using a precast 10% polyacrylamide gel. After the fixation of proteins in AcOH/MeOH/H_2O (1:4:5) for 30 min at room temperature and the washing with water for 5 min (three times), labeled actin was detected with a fluorescent imaging analyzer (BIO-RAD molecular imager FX, excitation and detection filter for TRITC, low sample intensity mode, resolution = 100 μm) followed by CBB-staining.

4.4. Photolabeling experiments with photoaffinity fluorescent probes

Actin (0.10 nmol) and tubulin (0.10 nmol as a heterodimer) were incubated with aplyronine A photoaffinity derivative **26** (0.30 nmol, prepared by the Huisgen reaction as mentioned below) in 10 μL of G-buffer or BRB buffer [80 mM PIPES·Na (pH 6.9), 2 mM $MgCl_2$, 0.5 mM EGTA, 10 μM DAPI] for 1 h in a rotator at 4 °C (Fig. 2b). For competition experiments, ApA (**1**) (5 nmol) was added simultaneously. In the cases of photoaffinity fluorescent probes **6** and **7**, actin (0.20 nmol) in 22 μL of G-buffer (Fig. S2b) or actin/tubulin (0.20 nmol each) in 20 or 300 μL of BRB buffer (Fig. 2d, 2e) was incubated with probe (0.5 nmol) on ice for 30 min. For competition experiments, ApA (**1**) (12.5 nmol) was simultaneously added. The resulting mixture was irradiated with UV light (365 nm) for 15 min on ice, treated with equal volumes of 2 × SDS-buffer, and boiled for 5 min at 95 °C. SDS-PAGE and fluorescent imaging detection was performed as mentioned above with a half of the samples (10~20 μL). Densitometry of fluorescence proteins were performed using ImageJ software with the 75 kDa protein in the Precision Plus Protein™ Dual Xtra Standards (cat. #161-0377).

4.5. In solution digestion and fluorescent LC-MS analysis

After actin was photolabeled with ApA–PF (**6**) in G-buffer as mentioned above, samples were diluted to 500 μL with 25 mM NH_4HCO_3 aq., and the solution was concentrated to 30 μL by ultrafiltration (14,000 × *g*, 4 °C, 15 min, MWCO 10 kDa). This solvent exchange was repeated three times. For comparison, the same amount of photoreacted actin was denatured with 2 M guanidine at 37 °C for 1 h or treated with excess ApA (**1**) (25 eq.) at 4 °C for 30 min before ultrafiltration. To the resulting solution (~30 μL) was added 45 mM DTT in 25 mM NH_4HCO_3 aq. (0.5 μL), and the mixture was incubated at 50 °C for 15 min. The solution was reacted with 100 mM iodoacetamide in 25 mM NH_4HCO_3 aq. (0.5 μL) under shaking at room temperature for 15 min, and incubated with trypsin (1:100 w/w, #V5111, Promega, 100 ng/μL, 13 μL) at 37 °C for 17 h.[13] After 10% TFA (0.6 μL) was added, the solution was concentrated to ~2 μL by centrifugation evapolator, and loaded on a Develosil RP-AQUEOUS AR-5 HPLC column (1.5 mm I.D. × 150 mm) at 25 °C. A linear gradient of 10% to 70% aq. MeCN containing 0.05% TFA was applied for 40 min at a flow rate of 100 μL/min, with monitoring of fluorescence (λ_{ex} 565 nm / λ_{em} 580 nm). For comparison, the water adduct of ApA–PF (**6**) was prepared. Probe **6** (1 nmol) in DMSO (1 μL) was diluted with water (44 μL) on ice. After irradiation of UV_{365} for 15 min, the sample was concentrated to 2 μL, and analyzed by fluorescent LC-MS.

4.6. Molecular modeling studies

Molecular modeling studies of the actin–photoaffinity probe complexes were performed using the Molecular Operating Environment (MOE) 2014.09 program package (Chemical Computing Group Inc.), as mentioned previously.[13] For docking model studies, water molecules associated with the actin–ApA (**1**) complex [PDB: 1WUA] were removed, and all protons on the protein and the ligand were complemented. The C34 *N*-methyl enamide moiety in **1** was replaced with the linker part of photoaffinity probes. Conformational search was performed using the Amber12:EHT force-field with GB/VI Generalized Born [26]

implicit solvent electrostatics (D_{in} = 1, D_{out} = 80). LowModeMD [27] was used for a conformational search, in which both the actin and the ApA moiety (C1–C34) in photoaffinity probes were fixed.

4.7. Spectroscopic analysis and general synthetic procedure

NMR spectra were recorded on a Bruker Biospin AVANCE 600 spectrometer (600 MHz for ^{1}H and 150 MHz for ^{13}C) or a Bruker Biospin AVANCE 400 spectrometer (400 MHz for ^{1}H and 100 MHz for ^{13}C). Chemical shifts are reported in parts per million (ppm) relative to the solvent peaks, δ_H 3.31 (residual C*H*D$_2$OD) and δ_C 49.0 for *C*D$_3$OD, respectively. Coupling constants (*J*) were shown in hertz. For the quantification of minute amounts by ^{1}H NMR analyses, benzene (5–10 mM in CD$_3$OD) was added to the sample solutions as a standard (1:60, v/v). IR spectra were recorded on a JASCO FT/IR-230 spectrometer. High-resolution electrospray ionization mass spectra (HR-ESIMS) were measured on an AccuTOF CS spectrometer (JEOL). LC-MS analysis was conducted using a Shimadzu LCMS-2020 single quadrupole mass spectrometer instrument with a fluorescence detector RF-20A. All chemicals were used as obtained commercially unless otherwise noted. Organic solvents and reagents for moisture-sensitive reactions were distilled by the standard procedure. Fuji Silysia silica gels BW-820MH and FL60D were used for column chromatography. Merck precoated silica gel 60 F254 plates were used for thin layer chromatography (TLC).

4.7. Synthesis and spectroscopic data of new compounds

4.7.1. PEG-linked amide 10. A solution of amide **8** (9.2 mg, 16 μmol) [14] in a 1:1 mixture of dry CH_2Cl_2 and trifluoroacetic acid (1 mL) was stirred for 20 min at room temperature and azeotropically concentrated with toluene *in vacuo* to give crude amine (14.2 mg) as a TFA salt. To a stirred solution of the crude amine TFA salt in dry DMF (1 mL) were added succinyl ester **9** (16.2 mg, 31.3 μmol), [28] *N*-methylmorpholine (NMM, 2.9 μL, 26 μmol), and a 1 M solution of *N*,*N*-dimethyl-4-aminopyridine (DMAP) in DMF (4.8 μL, 4.8 μmol) under a nitrogen atmosphere. After being stirred for 14.5 h at room temperature, the resulting mixture was concentrated *in vacuo*. The crude material was purified with a SiO_2 column (1.1 g, benzene / acetone = 2/1, 1/1 to 0/1) to give PEG-linked amide **10** (12.6 mg, 88%) as a colorless oil. Compound **10**: TLC R_f= 0.74 (1:1 benzene/acetone); $[\alpha]_D^{25}$ +1.2 (*c* 0.91, $CHCl_3$); ^{1}H NMR (400 MHz, CD$_3$OD) δ 7.79 (dd, *J* = 7.4 Hz, 2H), 7.62 (d, *J* = 7.4 Hz, 2H), 7.39 (t, *J* = 7.4 Hz, 2H), 7.30 (t, *J* = 7.4 Hz, 2H), 4.50 (d, *J* = 6.6 Hz, 2H), 4.28–4.22 (m, 3H), 3.93 (br s, 1H), 3.61–3.47 (m, 12H), 3.34–3.22 (m, 6H), 3.10 (t, *J* = 6.7 Hz, 2H), 2.54–2.44 (m, 5H), 1.83–1.51 (m, 10H), 1.41 (s, 9H); ^{13}C NMR (100 MHz, CD$_3$OD) δ 175.0, 174.5, 174.1, 171.0, 160.1, 158.4, 144.9 (2C), 142.6 (2C), 128.9 (2C), 128.2 (2C), 126.1 (2C), 121.0 (2C), 80.6, 79.9, 76.5, 72.2, 71.5 (2C), 71.2 (2C), 69.9, 69.9, 68.5, 54.6, 48.3, 39.7, 38.7, 37.9, 32.4, 32.1, 32.0, 30.9, 30.4, 29.8, 29.5, 28.8 (3C), 24.1; IR ($CHCl_3$) 3586, 3019, 1684, 1653, 1507, 1419, 1212, 1046, 784, 669 cm^{-1}; HRMS (ESI) *m/z* 903.4507 (calcd for $C_{45}H_{64}N_6NaO_{12}$ $[M+Na]^+$, Δ –2.8 mmu).

4.7.2. PEG-linked diazirine 12. A solution of PEG-linked amide **10** (34.2 mg, 38.9 μmol) in a 1:1 mixture of dry CH_2Cl_2 and trifluoroacetic acid (2 mL) was stirred for 1 h at room temperature and azeotropically concentrated with toluene *in vacuo* to give crude amine (45.8 mg) as a TFA salt. To a stirred solution of the crude amine TFA salt (15.3 mg, 1/3 amount) in dry DMF (2 mL) were added diazirine succinyl ester **11** (49.7 mg, 152 μmol),[29] NMM (5 μL, 46 μmol) and a 1 M solution of DMAP in DMF (15.6 μL, 15.6 μmol) under a nitrogen atmosphere. After being stirred for 3.5 day at room temperature, the resulting mixture was azeotropically concentrated with toluene. The crude material was purified with a SiO_2 column (1.2 g, $CHCl_3$ / MeOH = 1/1 to 0/1) and a Develosil ODS-HG-5 HPLC column [ϕ 20 mm I.D. × 250 mm, 80% aq. MeOH at a flow rate of 5 mL/min, with monitoring at 254 nm (t_R = 31 min)] to give PEG-linked diazirine **12** (22.1 mg, 57%) as a colorless oil. Compound **12**: TLC R_f = 0.58 (4:1 chloroform/methanol); $[\alpha]_D^{25}$ +9.7 (*c* 1.2, $CHCl_3$); ^{1}H NMR (600 MHz, CD$_3$OD) δ 7.89 (d, *J* = 8.4 Hz, 2H), 7.79 (d, *J* = 7.6 Hz, 2H), 7.61 (d, *J* = 7.6 Hz, 2H), 7.39 (dd, *J* = 7.6, 7.4 Hz, 2H), 7.32 (dd, *J* = 7.6, 7.4 Hz, 2H), 7.30 (t, *J* = 8.4 Hz, 2H), 4.49 (d, *J* = 6.7 Hz, 2H), 4.28–4.22 (m, 3H), 3.93 (dd, *J* = 4.2, 2.6 Hz, 1H), 3.62–3.44 (m, 12H), 3.24–3.21 (m, 8H), 2.57–2.43 (m, 5H), 1.90–1.33 (m, 10H); ^{13}C NMR (150 MHz, CD$_3$OD) δ 175.0, 174.4, 174.1, 171.0, 168.7, 160.1, 144.8 (2C), 142.6 (2C), 137.3, 133.0, 129.0 (2C), 128.9 (2C), 128.2 (2C), 127.7 (2C), 126.1 (2C), 123.4 (q, $^1J_{C-F}$ = 273 Hz), 121.0 (2C), 80.6, 76.5, 72.2, 71.5, 71.5, 71.2, 71.2, 70.2, 69.9, 68.5, 54.6, 48.2, 39.7, 38.8, 37.9, 32.4, 32.0, 32.0, 30.4, 30.3, 29.8, 29.5, 29.4 (q, $^2J_{C-F}$ = 40.5 Hz), 24.1; IR ($CHCl_3$) 3566, 3019, 2360, 1653, 1520, 1219, 929, 670 cm^{-1}; HRMS (ESI) *m/z* 1015.4159 (calcd for $C_{49}H_{59}F_3N_8NaO_{11}$ $[M+Na]^+$, Δ +0.6 mmu).

4.7.3. PEG-linked alkoxyamine 13. A solution of PEG-linked amide **12** (2.2 mg, 2.2 μmol) in a 4:1 mixture of dry DMF and piperidine (1 mL) was stirred at room temperature for 4.5 h. The reaction mixture was azeotropically concentrated with toluene to give alkoxyamine **13** (quant. monitored by TLC analysis), which was immediately used for the next step without further purification.

4.7.4. ApA–PPA (5). Aplyronine A (**1**) was isolated from the sea hare *Aplysia kurodai*, as described previously.[3] A solution of **1** (0.32 mg, 300 nmol) in a 3:1 mixture of 1,4-dioxane (150 μL) and 2 M aq. HCl (50 μL) was stirred for 1 h at 50 °C. The resulting mixture was diluted with sat. $NaHCO_3$ aq. (250 μL) and water (2 mL), and extracted with $CHCl_3$ (1 mL × 5). The combined extracts were washed with brine and concentrated to give aldehyde **25** (quant. monitored by HPTLC analysis: R_f 0.49, $CHCl_3$/MeOH = 9/1), which was used for the next step without further purification.

A solution of the aldehyde **25** and the alkoxyamine **13** prepared as above in a 9:1 mixture of EtOH and 50 mM

acetate buffer (pH 4.0) (0.3 mL) was stirred at room temperature for 156 h. The reaction mixture was directly applied twice to a Develosil ODS-HG-5 HPLC column (ϕ 20 mm I.D. × 250 mm). Samples were eluted with MeOH / 20 mM ammonium acetate (79:21) at a flow rate of 1 mL/min, with monitoring at 254 nm (t_R = 62 min) to give ApA–PPA (**5**) (73 nmol, 24%, based on NMR quantification, *E*/*Z* = 4/1 for the C34 isomers). The purified compound **5** was freeze-dried, dissolved in water, and freeze-dried again twice to remove remaining ammonium acetate. Compound **5**: ^{1}H NMR (600 MHz, CD_3OD) δ 7.89 (d, *J* = 8.1 Hz, 2H), 7.57 [6.86][1] (t, *J* = 6.1 Hz, 1H), 7.34 (d, *J* = 8.1 Hz, 2H), 7.20 (dd, *J* = 15.7, 10.6 Hz, 1H), 6.38 [6.38][2] (dd, *J* = 15.4, 11.0 Hz, 1H), 6.22 (m, 1H), 5.97 (d, *J* = 15.7 Hz, 1H), 5.64 (dt, *J* = 14.4, 10.2 Hz, 1H), 5.55 (d, *J* = 11.2 Hz, 1H), 5.10 (m, 1H), 4.80 (m, 1H), 4.68 (m, 1H), 4.41 [4.46][2] (s, 2H), 4.25 (m, 1H), 3.98–3.90 (m, 2H), 3.69–3.48 (m, 11H), 3.49–3.45 (m, 4H), 3.40 (m, 1H), 3.39–3.13 (m, 10H), 3.24 (s, 3H), 3.22 [3.22][2] (s, 3H), 3.18 (s, 2H), 3.15 (s, 3H), 3.08 (dd, *J* = 12.0, 8.1 Hz, 1H), 2.58–2.41 (m, 6H), 2.38 [2.39][2] (s, 6H), 2.34 [2.35][1] [2.33][3] (s, 6H), 2.41–2.27 (m, 2H), 2.27–2.10 (m, 2H), 2.10–1.93 (m, 1H), 2.04 [2.05][1, 3] [2.03][3] (s, 3H), 1.93–1.79 (m, 2H), 1.72 (dd, *J* = 6.7, 6.5 Hz, 1H), 1.64–1.56 (m, 2H), 1.56–1.45 (m, 5H), 1.50 [1.51][3] (s, 3H), 1.30 [1.33][3] (d, *J* = 6.8 Hz, 3H), 1.31 (m, 1H), 1.18–1.04 (m, 5H), 1.04–0.95 (m, 21H), 0.95–0.84 (m, 10H), 0.79–0.73 (m, 3H). Chemical shifts of the minor diastereomers are within parentheses as follows: []^1, 4:1 at C34 stereoisomers; []^2, 1.4:1 at C7 trimethylserine moiety; []^3, 1.2:1 at C29 dimethylalanine moiety; HRMS (ESI) *m/z* 1788.0560 (calcd for $C_{91}H_{146}F_3N_{10}O_{22}$ $[M+H]^+$, Δ –0.5 mmu).

4.7.5. Triazole 26. To a solution of ApA–PPA (**5**) (18 μg, 10 nmol) and 5-TAMRA azide (11 μg, 20 nmol, Thermo Fisher Scientific Inc., Cat. No. T10182) in a 1:12:12 mixture of DMSO–CH_2Cl_2–H_2O (250 μL) were added aqueous solutions of sodium ascorbate (100 mM, 1.5 μL) and copper sulfate (100 mM, 1.0 μL), and a solution of tris[(1-benzyl-*1H*-1,2,3-triazol-4-yl)methyl]amine (TBTA) [23] (100 mM, 1.0 μL) in DMSO. After being stirred at room temperature for 48 h, the resulting mixture was concentrated and purified by HPLC [Develosil ODS-HG-5 (ϕ 4.6 mm I.D. × 250 mm), MeOH / 20 mM ammonium acetate (82:18), 1 mL/min, UV 254 nm, λ_{ex} 565 nm, λ_{em} 580 nm] to give triazole **26** (1.9 nmol, 19%, t_R = 17 min). Compound **26**: HRMS (ESI) *m/z* 1193.6426 (calcd for $C_{122}H_{179}F_3N_{16}Na_2O_{26}$ $[M+2Na]^{2+}$, Δ –3.0 mmu).

4.7.6. TAMRA Boc amide 24. To a stirred solution of 5(6)-TAMRA succinimidyl ester (**23**) (5.1 mg, 9.7 μmol, purchased from Setareh Biotech LLC, 5-TAMRA/6-TAMRA = 4:1) in dry DMF (1 mL) were added 6-[(*tert*-butoxycarbonyl)amino]-1-hexylamine (21 mg, 95 μmol) and a 1 M solution of DMAP in DMF (19 μL, 19 μmol) under a nitrogen atmosphere. After being stirred for 94 h at room temperature, the resulting mixture was azeotropically concentrated with toluene. The crude material was purified with a SiO_2 column (1 g, $CHCl_3$ / MeOH = 1/0, 40/1, 20/1, 10/1, 5/1 to 1/1) and an ODS column (1 g, 70 to 100% aq. MeOH) to give TAMRA Boc amide **24** (5.8 mg, 97%, 5-TAMRA/6-TAMRA = 3.3:1). Compound **24**: ^{1}H NMR (400 MHz, CD_3OD) [5-TAMRA isomer] δ 8.77 (d, *J* = 1.8 Hz, 1H), 8.25 (dd, *J* = 1.8, 7.9 Hz, 1H), 7.51 (d, *J* = 7.9 Hz, 1H), 7.13 (d, *J* = 9.5 Hz, 2H), 7.03 (dd, *J* = 9.5, 2.3 Hz, 2H), 6.93 (d, *J* = 2.3 Hz, 2H), 3.46 (t, *J* = 7.2 Hz, 2H), 3.34 (s, 12H), 3.04 (t, *J* = 6.9 Hz, 2H), 1.73–1.30 (m, 14H), 1.40 (s, 9H); [6-TAMRA isomer] δ 8.39 (d, *J* = 8.2 Hz, 1H), 8.19 (dd, *J* = 1.8, 8.2 Hz, 1H), 7.82 (d, *J* = 1.8 Hz, 1H), 7.14 (d, *J* = 9.5 Hz, 2H), 7.03 (dd, *J* = 9.5, 2.3 Hz, 2H), 6.93 (d, *J* = 2.3 Hz, 2H), 3.37 (t, *J* = 7.2 Hz, 2H), 3.34 (s, 12H), 2.99 (t, *J* = 7.0 Hz, 2H), 1.73–1.30 (m, 14H), 1.42 (s, 9H); ^{13}C NMR (100 MHz, CD_3OD) [5-TAMRA isomer] δ 168.9, 168.2, 161.5, 159.9 (2C), 159.8 (2C), 159.5, 138.9, 138.9, 138.7, 133.1, 132.9, 132.8 (2C), 132.2, 116.4 (2C), 115.6 (2C), 98.3 (2C), 80.7, 42.1, 42.0, 41.8 (4C), 31.8, 31.2, 29.7 (3C), 28.6, 28.4; [6-TAMRA isomer] δ 168.6, 168.2, 161.4, 159.9 (2C), 159.8 (2C), 159.5, 140.4, 136.4, 135.9, 133.7, 132.8 (2C), 131.2, 130.8, 116.4 (2C), 115.7 (2C), 98.3 (2C), 80.7, 42.1, 42.0, 41.8 (4C), 31.8, 31.1, 29.7 (3C), 28.5, 28.3; IR ($CHCl_3$) 1704, 1649, 1596, 1535, 1491, 1420, 1187, 1138, 764, 754 cm^{-1}; HRMS (ESI) *m/z* 629.3334 (calcd for $C_{36}H_{46}N_4O_6$ $[M+H]^+$, Δ +0.0 mmu).

4.7.7. TAMRA amine 16. A solution of TAMRA Boc amide **24** (4.8 mg, 7.6 μmol, 5-TAMRA/6-TAMRA = 1.3:1) in a 1:1 mixture of dry CH_2Cl_2 and trifluoroacetic acid (2 mL) was stirred for 40 min at room temperature and azeotropically concentrated with toluene *in vacuo* to give crude amine **16** (5.0 mg, quant.) as a TFA salt, which was immediately used for the next step without further purification.

4.7.8. NHS ester 15. To a stirred solution of carboxylic acid **14** (42 mg, 77 μmol) [30] in dry CH_2Cl_2 (0.4 mL) was added *N*-hydroxysuccimide (8.9 mg, 77 μmol) and a 0.25 M solution of *N*,*N'*-dicyclohexylcarbodiimide in dry CH_2Cl_2 (0.4 mL, 100 μmol). After stirring at room temperature for 4 h, the reaction mixture was filtered through a cotton wool plug, and the filtrate was concentrated *in vacuo* to give crude NHS ester **15** (44 mg) as a colorless powder, which was immediately used for the next step without further purification.

4.7.9. TAMRA-linked Boc amide 17. To a mixture of the amine TFA salt **16** (5.0 mg, 7.6 μmol), the NHS ester **15** (22 mg, ~34 μmol, half amount of the above sample) in dry DMF (0.6 mL) were added a 10% solution of NMM in DMF (17 μL, 15 μmol), and a 0.1 M solution of DMAP in DMF (7.6 μL, 0.76 μmol) under a nitrogen atmosphere. After being stirred for 18 h at room temperature, the resulting mixture was concentrated *in vacuo*. The crude material was purified with a SiO_2 column (1 g, $CHCl_3$/MeOH = 1/0, 49/1, 19/1, 9/1, 4/1, 2/1) to give TAMRA-linked Boc amide **17** (6.0 mg, 74% from amine **16**, 5-TAMRA/6-TAMRA = 1.4/1.0) as a brownish oil. Compound **17**: R_f 0.66 and 0.63 (4:1 $CHCl_3$/MeOH); $[\alpha]_D^{25}$ –2190 (*c* 0.15, $CHCl_3$); ^{1}H NMR (400 MHz, CD_3OD) [5-TAMRA isomer] δ 8.77 (d, *J* = 1.8 Hz, 1H), 8.26 (dd, *J* = 1.8, 8.1 Hz, 1H), 7.77 (br d, *J* = 7.4 Hz, 2H), 7.58 (br d, *J* = 7.5 Hz, 2H), 7.47 (d, *J* = 8.1 Hz, 1H), 7.36 (dt, *J* = 3.9, 7.4 Hz, 2H), 7.27 (t, *J* = 7.4 Hz, 2H), 7.09 (d, *J* = 9.4 Hz, 2H),

7.00 (dd, *J* = 2.5, 9.4 Hz, 2H), 6.93 (d, *J* = 2.5 Hz, 2H), 4.46 (d, *J* = 6.5 Hz, 2H), 4.22 (s, 2H), 4.16 (t, *J* = 6.5 Hz, 1H), 4.00 (m, 1H), 3.50–3.10 (m, 6H), 3.27 (s, 12H), 1.79–1.29 (m, 14H), 1.39 (s, 9H); [6-TAMRA isomer] δ 8.39 (d, *J* = 8.2 Hz, 1H), 8.19 (dd, *J* = 1.7, 8.2 Hz, 1H), 7.82 (d, *J* = 1.7 Hz, 1H) , 7.77 (br d, *J* = 7.4 Hz, 2H), 7.58 (br d, *J* = 7.5 Hz, 2H), 7.36 (dt, *J* = 3.9, 7.4 Hz, 2H), 7.27 (t, *J* = 7.4 Hz, 2H), 7.10 (d, *J* = 9.4 Hz, 2H), 7.00 (dd, *J* = 2.5, 9.4 Hz, 2H), 6.92 (d, *J* = 2.5 Hz, 2H), 4.44 (d, *J* = 6.5 Hz, 2H), 4.19 (s, 2H), 4.16 (t, *J* = 6.5 Hz, 1H), 3.93 (m, 1H), 3.50–3.10 (m, 6H), 3.27 (s, 12H), 1.79–1.29 (m, 14H), 1.41 (s, 9H); ^{13}C NMR (100 MHz, CD_3OD) [purified 5-TAMRA isomer] δ 174.7, 172.1, 169.5, 162.3, 161.1, 161.0, 159.9 (2C), 159.7 (2C), 159.3, 145.8 (2C), 145.6 (2C), 143.4 (2C), 138.4, 133.1, 132.2, 131.6, 131.3, 129.8 (2C), 129.1 (2C), 127.0 (2C), 126.9 (2C), 121.9 (2C), 116.1 (2C), 115.6 (2C), 98.2 (2C), 80.7, 77.5, 69.6, 55.5, 50.7, 49.0, 41.9, 41.7 (4C), 41.0, 33.8, 31.4, 31.2, 31.1, 29.6 (3C), 28.3, 28.2; IR ($CHCl_3$) 1650, 1597, 1520, 1490, 1348, 1209, 1187, 1137, 671 cm^{-1}; HRMS (ESI) *m/z* 1052.5133 (calcd for $C_{59}H_{70}N_7O_{11}$ $[M+H]^+$, Δ +0.5 mmu).

4.7.10. Diazirine 19. Prepared from Boc amide **17** (6.0 mg, 5.7 μmol, 5/6-TAMRA = 1.4/1.0) and diazirine succinyl ester **11** (7.5 mg, 23 μmol) in 39% yield using the same procedure as that for **12**. Compound **19**: t_R = 29–33 min [Develosil ODS-HG-5, ϕ 20 × 250 mm, MeOH / 0.1% TFA (79/21), 5 mL/min, UV 254 nm, 5/6-TAMRA = 1.4/1.0]; ^{1}H NMR (400 MHz, CD_3OD) [5-TAMRA isomer] δ 8.76 (d, *J* = 1.8 Hz, 1H), 8.25 (dd, *J* = 1.8, 7.9 Hz, 1H), 7.91 (d, *J* = 8.4 Hz, 2H), 7.75 (br d, *J* = 7.5 Hz, 2H), 7.56 (br d, *J* = 7.5 Hz, 2H), 7.45 (d, *J* = 7.9 Hz, 1H), 7.35 (t, *J* = 7.5 Hz, 2H), 7.29 (d, *J* = 8.4 Hz, 2H), 7.25 (t, *J* = 7.5 Hz, 2H), 7.09 (d, *J* = 9.4 Hz, 2H), 7.02 (dd, *J* = 2.4, 9.4 Hz, 2H), 6.94 (d, *J* = 2.4 Hz, 2H), 4.36 (dd, *J* = 5.8, 8.4 Hz, 1H), 4.41 (d, *J* = 6.4 Hz, 2H), 4.20 (s, 2H), 4.12 (t, *J* = 6.4 Hz, 2H), 3.50–3.10 (m, 6H), 3.34 (s, 12H), 1.95–1.30 (m, 14H); [6-TAMRA isomer] δ 8.38 (d, *J* = 8.5 Hz, 1H), 8.18 (dd, *J* = 1.7, 8.5 Hz, 1H), 7.88 (d, *J* = 8.4 Hz, 2H), 7.83 (d, *J* = 1.7 Hz, 1H), 7.75 (br d, *J* = 7.5 Hz, 2H), 7.56 (br d, *J* = 7.5 Hz, 2H), 7.34 (t, *J* = 7.5 Hz, 1H), 7.28 (d, *J* = 8.4 Hz, 2H), 7.25 (t, *J* = 7.5 Hz, 2H), 7.09 (d, *J* = 9.4 Hz, 2H), 6.99 (dd, *J* = 2.4, 9.4 Hz, 2H), 6.91 (d, *J* = 2.4 Hz, 2H), 4.42 (d, *J* = 6.4 Hz, 2H), 4.39 (dd, *J* = 6.0, 8.5 Hz, 1H), 4.18 (s, 2H), 4.12 (t, *J* = 6.4 Hz, 2H), 3.50–3.10 (m, 6H), 3.34 (s, 12H), 1.95–1.30 (m, 14H); HRMS (ESI) *m/z* 1164.4786 (calcd for $C_{63}H_{65}F_3N_9O_{10}$ $[M+H]^+$, Δ –1.5 mmu).

4.7.11. Alkoxyamine 20. A solution of diazirine **19** (1.0 mg, 0.86 μmol) in a 4:1 mixture of dry DMF and diethylamine (0.5 mL) was stirred at room temperature for 5 min. The reaction mixture was azeotropically concentrated with toluene to give alkoxyamine **20** (quant. monitored by TLC analysis), which was immediately used for the next step without further purification.

4.7.12. ApA–PF (6). Prepared from aplyronine A (**1**) (0.21 mg, 200 nmol) and alkoxyamime **20** (0.86 μmol, prepared as above) in 41% yield (isolated as 5-TAMRA isomer) using the same procedure as that for **5**. Compound **6**: t_R = 27–30 min [Develosil ODS-HG-5, ϕ 20 × 250 mm, MeOH / 20 mM NH_4OAc aq. (85/15), 5 mL/min, UV = 254 nm]; ^{1}H NMR (600 MHz, CD_3OD) δ 8.50 (d, *J* = 1.7 Hz, 1H), 8.03 (dd, *J* = 1.7, 7.4 Hz, 1H), 7.97 (d, *J* = 8.2 Hz, 2H), 7.53 [6.79]^1 (t, *J* = 7.0 Hz, 1H), 7.34 (d, *J* = 7.4 Hz, 1H), 7.32 (d, *J* = 8.2 Hz, 2H), 7.24 (dd, *J* = 2.2, 9.5 Hz, 2H), 7.19 (dd, *J* = 11.0, 15.4 Hz, 1H), 7.01 (dd, *J* = 2.3, 9.5 Hz, 2H), 6.93 (br s, 2H), 6.37 (m, 1H), 6.21 (m, 1H), 5.96 (d, *J* = 15.4 Hz, 1H), 5.63 (m, 1H), 5.54 (br d, *J* = 11.0 Hz, 1H), 5.34 (m, 1H), 4.95–4.80 (m, 3H), 5.09 (m, 1H), 4.96 (m, 1H), 4.77 (m, 1H), 4.47 (dd, *J* = 5.5, 9.2 Hz, 1H), 4.37 [4.43]^1 (s, 2H), 3.70–3.22 (m, 16H), 3.63 (s, 12H), 3.17 (s, 3H), 3.14 (s, 3H), 3.07 (m, 1H), 2.37 [2.38]^2 (s, 6H), 2.33 [2.32]^1 [2.34]^3 [2.32]^{1,3} (s, 6H), 2.50–2.25 (m, 4H), 2.02 [2.03]^1 [2.01]^3 [2.02]^{1,3} (s, 3H), 2.16–1.13 (m, 36H), 1.51 [1.52]^2 (s, 3H), 1.02 (d, *J* = 6.7 Hz, 3H), 1.01–0.93 (m, 15H), 0.76 (m, 3H). Chemical shifts of the minor diastereomers are within parentheses as follows: []^1, 7:3 at C34 stereoisomers; []^2, 1.5:1 at C7 trimethylserine moiety; []^3, 1.2:1 at C29 dimethylalanine moiety; HRMS (ESI) *m/z* 991.0452 (calcd for $C_{105}H_{151}F_3N_{11}NaO_{21}$ $[M+H+Na]^{2+}$, Δ –1.0 mmu).

4.7.13. PEG-linked amide 18. Prepared from Boc amide **17** (3.2 mg, 3.0 μmol, 5/6-TAMRA = 3.2/1.0) and succinyl ester **9** (16 mg, 35 μmol) in 63% yield (5/6-TAMRA = 3.2/1.0) using the same procedure as that for **10**. 5-TAMRA isomer **18** and its 6-TAMRA isomer were separated by HPLC. Compound **18**: t_R = 59–64 min [Develosil ODS-HG-5, ϕ 20 × 250 mm, MeOH / 0.1% TFA (68/32), 5 mL/min, UV 254 nm]; $[\alpha]_D^{25}$ –60 (*c* 0.45, $CHCl_3$); ^{1}H NMR (400 MHz, CD_3OD) δ 8.77 (d, *J* = 1.8 Hz, 1H), 8.28 (dd, *J* = 7.9, 1.8 Hz, 1H), 7.77 (d, *J* = 7.5 Hz, 2H), 7.58 (d, *J* = 7.5 Hz, 2H), 7.47 (d, *J* = 7.9 Hz, 1H), 7.36 (t, *J* = 7.5 Hz, 2H), 7.27 (t, *J* = 7.5 Hz, 2H), 7.10 (d, *J* = 9.5 Hz, 2H), 7.01 (dd, *J* = 9.5, 2.1 Hz, 2H), 6.94 (d, *J* = 2.1 Hz, 2H), 4.45 (d, *J* = 6.6 Hz, 2H), 4.24 (m, 1H), 4.23 (s, 2H), 4.17 (t, *J* = 6.6 Hz, 1H), 3.61–3.55 (m, 4H), 3.55–3.50 (m, 4H), 3.49–3.45 (m, 6H), 3.27 (s, 12H), 3.26–3.20 (m, 8H), 2.55–1.25 (m, 22H), 1.41 (s, 9H); ^{13}C NMR (100 MHz, CD_3OD) δ 175.1, 174.4, 174.3, 171.0, 168.1, 167.4, 160.7, 160.1 (2C), 159.0 (4C), 144.9 (2C), 142.6 (2C), 138.0 (2C), 137.9, 132.8, 132.3, 131.9 (2C), 131.3, 129.0 (2C), 128.2 (2C), 126.1 (2C), 121.1 (2C), 115.6 (2C), 114.7 (2C), 97.5 (2C), 79.9, 76.6, 71.6, 71.2, 69.9 (2C), 68.6, 55.0, 49.7, 48.3, 41.0, 40.9 (5C), 40.2, 39.7, 38.7, 37.9, 32.4, 32.1, 32.0, 30.9, 30.4, 30.3, 30.2, 29.8, 28.8 (3C), 27.5, 27.4, 24.3; IR ($CHCl_3$) 3674, 3344, 3006, 2932, 2870, 1651, 1598, 1537, 1349, 1251, 1188, 1138, 930, 826 cm^{-1}; HRMS (ESI) *m/z* 688.8401 (calcd for $C_{73}H_{96}N_9NaO_{16}$ $[M+H+Na]^{2+}$, Δ –3.0 mmu).

4.7.14. PEG-linked diazirine 21. Prepared from Boc amide **18** (1.0 mg, 0.73 μmol) and diazirine succinyl ester **11** (1.0 mg, 3.1 μmol) in 61% yield using the same procedure as that for **12**. Compound **21**: R_f = 0.34 (MeOH / 0.1% TFA aq. = 90/10, ODS-W); ^{1}H NMR (400 MHz, CD_3OD) δ 8.77 (d, *J* = 1.8 Hz, 1H), 8.26 (dd, *J* = 7.9 Hz, 1.8 Hz, 1H), 7.87 (d, *J* = 8.2 Hz, 2H), 7.76 (d, *J* = 7.5 Hz, 2H), 7.58 (d, *J* = 7.5 Hz, 2H), 7.47 (d, *J* = 7.9 Hz, 1H), 7.36 (t, *J* = 7.5 Hz, 2H), 7.30 (d, *J* = 8.2 Hz, 2H), 7.27 (t, *J* = 7.5 Hz, 2H), 7.10 (d, *J* = 9.5 Hz, 2H), 7.01 (dd, *J* = 9.5, 2.4 Hz,

2H), 6.93 (d, J = 2.4 Hz, 2H), 4.45 (d, J = 6.7 Hz, 2H), 4.23 (m, 1H), 4.21 (s, 2H), 4.16 (t, J = 6.7 Hz, 1H), 3.64–3.55 (m, 4H), 3.55–3.49 (m, 4H), 3.49–3.38 (m, 6H), 3.27 (s, 12H), 3.24–3.15 (m, 8H), 2.56–2.39 (m, 4H), 1.90–1.20 (m, 18 H); HRMS (ESI) *m/z* 755.8147 (calcd for $C_{77}H_{90}F_3N_{11}Na_2O_{15}$ $[M+2Na]^{2+}$, Δ –3.0 mmu).

4.7.15. PEG-linked alkoxyamine 22. Prepared from diazirine **21** (0.4 mg, 0.32 μmol) using the same procedure as that for **20**, which was immediately used for the next step without further purification.

4.7.16. ApA–PPF (7). Prepared from aplyronine A (**1**) (0.11 mg, 100 nmol) and alkoxyamime **22** (0.32 μmol) in 61% yield using the same procedure as that for **5**. Compound **7**: t_R = 70−79 min [Develosil ODS-HG-5, ϕ 20 × 250 mm, MeOH/0.1% TFA = 79/21, 5 mL/min, UV = 254 nm]; ^{1}H NMR (600 MHz, CD_3OD) δ 8.50 (d, J = 1.8 Hz, 1H), 8.04 (dd, J = 7.8, 1.8 Hz, 1H), 7.88 (d, J = 8.5 Hz, 2H), 7.55 [6.86]^1 (t, J = 6.5 Hz, 1H), 7.34 (d, J = 7.8 Hz, 2H), 7.31 (d, J = 8.5 Hz, 2H), 7.24 (d, J = 9.5 Hz, 2H), 7.21 (dd, J = 15.4, 11.0 Hz, 1H), 7.00 (dd, J = 9.5, 2.4 Hz, 2H), 6.90 (d, J = 2.4 Hz, 2H), 6.37 (m, 1H), 6.22 (m, 1H), 5.96 (d, J = 15.4 Hz, 1H), 5.63 (ddd, J = 14.6, 10.6, 4.0 Hz, 1H), 5.54 (br d, J = 11.2 Hz, 1H), 5.10–5.07 (m, 2H), 4.40 [4.46]^1 (s, 2H), 4.30–3.90 (m, 4H), 3.70–3.50 (m, 15H), 3.50−3.42 (m, 7H), 3.37 (s, 3H), 3.37–3.35 (m, 2H), 3.27 (s, 12H), 3.25–3.15 (m, 12H), 3.14 (s, 3H), 3.05 (br d, J = 9.0 Hz, 1H), 2.60–2.40 (m, 5H), 2.37 [2.38]^2 (s, 6H), 2.33 [2.32]^3 (s, 6H), 2.40–2.10 (m, 4H), 2.03 (s, 3H), 2.20–1.95 (m, 8H), 1.90–1.20 (m, 36H), 1.51 (s, 3H), 1.20–0.90 (m, 20H), 0.76 (d, J = 8.5 Hz, 3H). Chemical shifts of the minor diastereomers are within parentheses as follows: []^1, 7:3 at C34 stereoisomers; []^2, 1.5:1 at C7 trimethylserine moiety; []^3, 1.3:1 at C29 dimethylalanine moiety; HRMS (ESI) *m/z* 1142.6405 (calcd for $C_{77}H_{91}F_3N_{11}NaO_{15}$ $[M+H+Na]^{2+}$, Δ +0.5 mmu).

Acknowledgements

We thank Prof. Takeo Usui (University of Tsukuba) for his valuable suggestions regarding the purification and biochemical experiments of tubulin. This work is supported in part by JSPS grants (25702047 to M.K. and 26242073 to H.K.). Supports were also provided by PRESTO, JST (JPMJPR1535), and the Naito Foundation.

Supplementary data

Supplementary data associated with this article can be found, in the online version, at http://dx.doi.org/10.1016/j.bmc.2017.??.???.

References and notes

1. Milroy, L. –G.; Grossmann, T. N.; Hennig, S.; Brunsveld, L.; Ottmann, C. *Chem. Rev.* **2014**, *114*, 4695–4748.
2. Bovens, S.; Ottmann, C. in *Chemical Biology: Learning through Case Studies* (Eds., Waldmann, H.; Jannig, P.). Wiley–VCH Verlag GmbH, Weinheim, **2009**, pp. 105–119.
3. Yamada, K.; Ojika, M.; Ishigaki, T.; Yoshida, Y.; Ekimoto, H.; Arakawa, M. *J. Am. Chem. Soc.* **1993**, *115*, 11020–11021.
4. Ojika, M.; Kigoshi, H.; Ishigaki, T.; Tsukada, I.; Tsuboi, T.; Ogawa, T.; Yamada, K. *J. Am. Chem. Soc.* **1994**, *116*, 7441–7442.
5. Yamada, K.; Ojika, M.; Kigoshi, H.; Suenaga, K. *Nat. Prod. Rep.* **2007**, *26*, 27–43.
6. Kita, M.; Kigoshi, H. *Nat. Prod. Rep.* **2015**, *32*, 534–542.
7. Kita, M.; Kigoshi, H. *J. Synth. Org. Chem. Jpn.* **2015**, *73*, 151–160.
8. Saito, S.; Watabe, S.; Ozaki, H.; Kigoshi, H.; Yamada, K.; Fusetani, N.; Karaki, H. *J. Biochem.* (Tokyo) **1996**, *120*, 552–555.
9. Kita, M.; Hirayama, Y.; Sugiyama, M.; Kigoshi, H. *Angew. Chem. Int. Ed.* **2011**, *50*, 9871–9874.
10. Hirayama, Y.; Yamagishi, K.; Suzuki, T.; Kawagishi, H.; Kita, M.; Kigoshi, H. *Bioorg. Med. Chem.* **2016**, *24*, 2809–2814.
11. Kita, M.; Yoneda, K.; Hirayama, Y.; Yamagishi, K.; Saito, Y.; Sugiyama, Y.; Miwa, Y.; Ohno, O.; Morita, M.; Suenaga, K.; Kigoshi, H. *ChemBioChem* **2012**, *13*, 1754–1758.
12. Yoneda, K.; Hu, Y.; Kita, M.; Kigoshi, H. *Sci. Rep.* **2015**, *5*, 17853.
13. Yoneda, K.; Hu, Y.; Watanabe, R.; Kita, M.; Kigoshi, H. *Org. Biomol. Chem.* **2016**, *14*, 8564–8569.
14. Kita, M.; Hirayama, Y.; Yamagishi, K.; Yoneda, K.; Fujisawa, R.; Kigoshi, H. *J. Am. Chem. Soc.* **2012**, *134*, 20314–20317.
15. Kita, M.; Hirayama, Y.; Yoneda, K.; Yamagishi, K.; Chinen, T.; Usui, T.; Sumiya, E.; Uesugi, M.; Kigoshi, H. *J. Am. Chem. Soc.* **2013**, *135*, 18089–18095.
16. Rodriguez, O. C.; Schaefer, A. W.; Mandato, C. A.; Forscher, P.; Bement, W. M.; Waterman–Storer, C. M. *Nat. Cell Biol.* **2003**, *5*, 599–609.
17. Jordan, M. A.; Wilson, L. *Nat. Rev. Cancer* **2004**, *4*, 253–265.
18. Dumontet, C.; Jordan, M. A. *Nat. Rev. Drug Discov.* **2010**, *9*, 790–803.
19. Nassal, M. *Liebigs Ann. Chem.* **1983**, 1510–1523.
20. Hatanaka, Y.; Kanaoka, Y. *Heterocycles* **1998**, *47*, 625–632.
21. Kolb, H. C.; Finn, M. G.; Sharpless, K. B. *Angew. Chem. Int. Ed.* **2001**, *40*, 2004–2021.
22. Hirata, K.; Muraoka, S.; Suenaga, K.; Kuroda, K.; Kato, K.; Tanaka, H.; Yamamoto, M.; Takata, M.; Yamada, K.; Kigoshi, H. *J. Mol. Biol.* **2006**, *356*, 945–954.
23. Chan, T. R.; Hilgraf, R.; Sharpless, K. B.; and Fokin, V. V. *Org. Lett.* **2004**, *6*, 2853–2855.
24. Brunner, J.; Serin, H.; Richards, F. M. *J. Biol. Chem.* **1980**, *255*, 3313–3318.
25. Castoldi, M.; Popov, A. V. *Protein Expr. Purif.* **2003**, *32*, 83–88.
26. Labute, P. *J. Comput. Chem.* **2008**, *29*, 1963–1968.
27. Labute, P. *J. Chem. Inf. Model.* **2010**, *50*, 792–800.
28. Rajopadhye, M.; Edwards, S. D.; Harris, T. D.; Heminway, S. J.; Liu, S.; Singh P., R. *PCT Int. Appl.* WO9958162.
29. Strømgaard, K.; Saito, R. D.; Shindou, H.; Ishii, S.; Shimizu, T.; Nakanishi, K. *J. Med. Chem.* **2002**, *45*, 4038–4046.
30. Clave, G.; Boutal, H.; Hoang, A.; Perraut, F.; Volland, H.; Renard, P. Y.; Romieu, A. *Org. Biomol. Chem.* **2008**, *6*, 3065−3078.